Applied Energy 210 (2018) 1280–1289

Contents lists available at ScienceDirect

Applied Energy

journal homepage: www.elsevier.com/locate/apenergy

Optimal residential community demand response scheduling in smart grid

Sibo Nan *, Ming Zhou, Gengyin Li

State Key Laboratory for Alternate Electrical Power System with Renewable Energy Sources, North China Electric Power University, No. 2 Beinong Road, Changping District, 102206 Beijing, China

HIGHLIGHTS

- Propose optimal scheduling scheme for smart residential community.
- Classify smart residential loads into different categories according to different demand response capabilities.
- Reduce the peak load and peak-valley difference of residential load profile without bringing discomfort to the users.
- Provide support for the decision of electricity pricing strategy under electric power market development.

ARTICLE INFO

Article history:
Received 28 March 2017
Received in revised form 19 May 2017
Accepted 19 June 2017
Available online 23 June 2017

Keywords:
Smart residential community
Controllable load
Distributed generation
Demand response

ABSTRACT

With the reformation of electric power market and the development of smart grid technology, smart residential community, a new residential demand side entity, tends to play an important role in demand response program. This paper presents a demand response scheduling model for the novel residential community incorporating the current circumstances and the future trends of demand response programs. In this paper, smart residential loads are firstly classified into different categories according to various demand response programs. Secondly, a complete scheduling scheme is modeled based on the dispatch of residential loads and distributed generation. The presented model reduces the cost of user's electricity consumption and decreases the peak load and peak-valley difference of residential load profile without bringing discomfort to the users, through which residential community can participate in demand response efficiently. Besides, this model can also provide support for the decision of electricity pricing strategies under power market development.

1. Introduction

Demand response (DR), the main method of interaction between the power grid and customers under power market development, has been widely applied in recent years. In perspective of the grid utility, DR can improve load profile by reducing peak load and peak-valley difference, thus decreasing the operation cost of the system, and alleviating the pressure of the grid investment on load increase. On the other hand, for the electricity consumers, DR reduces cost of customers' electricity consumption without affecting their satisfaction. Among loads that can participate in DR, residential load has great potentiality, and can effectively ameliorate the demand-side load curve [1,2].

With the development of smart grid technology, controllable loads and distributed generation (DG) have been gradually integrated into residential side. Smart meters, in addition, have been gradually applied to residential buildings. Therefore, a new DR participant with considerable load flexibility arises from residential side, which is smart residential community. Fig. 1 shows the components of the load and DG in smart residential community that include interruptible load, controllable load, roof-top solar panel, and storage battery. In comparison to conventional residential loads, smart residential community has greater DR potentiality leading to that it can smooth the load curve more dramatically owing to its load flexibility. In addition, DR of smart residential community is also crucial for ancillary service entities to get involved in power market. Since smart residential community arises freshly, few studies have been done upon DR of this specific entity. Thus, it is meaningful and necessary to study the DR strategy of smart residential community.

China has initiated numerous demonstration projects of smart residential community during the past several years aiming to reduce the peak load, load peak-valley difference and energy

* Corresponding author.
E-mail address: nansibo1988@163.com (S. Nan).

http://dx.doi.org/10.1016/j.apenergy.2017.06.066
0306-2619/

Nomenclature

Indices

l	superscript for interruptible load
a	superscript for adjustable load
b	superscript for shiftable load
i	index for power generation unit
j, k	index for load unit
t	index for time

Parameters

$P_j^{l,\max}$	maximum curtailable power of interruptible load j at each hour (kW)
$X_j^{l,\max}$	maximum daily curtailable hours of load j (h)
$P_{j,t}^{L}$	original load power of load j at hour t (kW)
$P_{j,t}^{a,base}$	original power of illumination load j at hour t (kW)
$\rho_j^{a,\min}$	price threshold of illumination load j (¥/kW h)
$P_{j,t}^{a,\min}$	adjusted power of illumination load j at hour t (kW)
ρ_t	power price of grid at hour t (¥/kW h)
ε	small positive constant (which equals to 0.001 in this paper)
$T_{k,t}^{\alpha}$	ambient temperature of air conditioner k at hour t (°C)
α_k	system inertia of air conditioner k
Δt	control interval (1 h)
C_k	thermal capacitance of air conditioner k (kW h/°C)
R_k	thermal resistance of air conditioner k (°C/kW)
η_k	working efficiency factor of air conditioner k
$P_k^{\min}$, $P_k^{\max}$	minimum and maximum power of air conditioner k at each hour (kW)
$T_{k,t}^{s,base}$	original temperature set point of air conditioner k at hour t (°C)
$T_{k,t}^{s,\max}$	adjusted temperature set point of air conditioner k at hour t in cooling mode (°C)
$\rho_k^{a,\min}$	price threshold of air conditioner k (¥/kW h)
$P_j^{b,average}$	average power of shiftable load j (kW)
$X_{j,t}^{b,on}$	total operated hours of shiftable load j at hour t (h)
U_j^b	cycle duration of shiftable load j (h)
τ	start hour of time window set by user (h)
T	end hour of time window set by user (h)
$P_k^{b,\min}$, $P_k^{b,\max}$	minimum and maximum charge power of EV k at each hour (kW)
T_a	users EV home arrival time (i.e. EV plug-in time) (h)
T_b	end of users EV charge time (h)
$E_k^{\max}$	battery capacity of EV k (kW h)
D	maximum mileage of EV
ρ_j^l	interruptible load curtailment tariff (¥/kW h)
$P^{g,\min}$, $P^{g,\max}$	minimum/maximum purchased power from grid at each hour (kW)
$P_{c,i}^{\min}$, $P_{c,i}^{\max}$	minimum/maximum charge power of battery i at each hour (kW)
$P_{d,i}^{\min}$, $P_{d,i}^{\max}$	minimum/maximum discharge power of battery i at each hour (kW)
η_i^S	discharge/charge inverter efficiency
$E_i^{\min}$, $E_i^{\max}$	minimum/maximum stored energy of battery i (kW h)
NT	total schedule hours (24 h in this paper)

Variables

$P_{j,t}^{l}$	curtailed power of user j at hour t (kW)
$I_{j,t}^{l}$	binary status indices of interruptible load j at hour t (if load is curtailed, $I_{j,t}^{l}=1$)
$P_{j,t}^{a}$	power of illumination load j at hour t (kW)
$I_{j,t}^{a}$	binary status indices of adjustment of illumination load j at hour t (when hourly price is higher than $\rho_{j,t}^{a,\min}$, $I_{j,t}^{a}=1$)
$T_{k,t}$	air conditioner temperature of air conditioner k at hour t (°C)
$T_{k,t}^{g}$	temperature adjustment of air conditioner k at hour t (°C) when it is turned on
$P_{k,t}^{a}$	load power of air conditioner k at hour t (kW)
$T_{k,t}^{s}$	temperature set point of air conditioner k at hour t (°C)
$I_{k,t}^{a}$	binary status indices of adjustment of air conditioner k at hour t (when hourly price is higher than $\rho_{k,t}^{a,\min}$, $I_{k,t}^{a}=1$)
$P_{j,t}^{b}$	load power of shiftable load j at hour t (kW)
$I_{j,t}^{b}$	binary status indices of shiftable load j at hour t (when load is on, $I_{j,t}^{b}=1$)
$P_{k,t}^{b}$	charge power of EV k at hour t (kW)
$I_{k,t}^{b}$	binary charge status indices of EV k at hour t (when EV is charged, $I_{k,t}^{b}=1$)
$E_{k,t}^{b}$	SOC of EV k at hour t
P_t^g	power purchased from grid at hour t (kW)
$P_{i,t}^{V}$	solar power generation of unit i at hour t (kW)
$P_{i,t}^{S}$	battery charge/discharge power of battery i at hour t (kW)
$P_{d,i,t}$,$P_{c,i,t}$	discharge power/charge power of battery i at hour t (kW)
$I_{d,i,t}$,$I_{c,i,t}$	discharge/charge binary status indices of battery i at hour t (when battery discharges/charges, $I_{d,i,t}=1/I_{c,i,t}=1$)
$E_{i,t}$	SOC of battery i at hour t

consumption in cities, and those projects are currently in high-speed progress. One of the projects has been conducted in Suzhou, Jiangsu Province, China, where the residential community participates in DR through advanced metering infrastructure (AMI) coordinated by load aggregator (LA). The DR structure of the community is shown in Fig. 2. Each particular interruptible load and controllable load of household is connected with smart meters. The smart meters record and transport the load data to LA, and delivers the scheduling signals from LA to controllers of each load such as smart plug, control module of air conditioner, etc. to realize the aggregation and direct dispatch of each load by LA. Time-of-use (TOU) and critical peak pricing (CPP) DR programs are currently considered to be tested on this community in different days, and the test of real time pricing (RTP) and interruptible loads (IL) programs are also concerned in the future. Therefore, this particular DR structure requests for a novel optimal scheduling tool to apply price-based and incentive-based DR programs, which dives and supports the work of this paper.

There are some researches on residential DR in recent years, most of which are from the United States and European countries. Ref. [3] presents a control strategy for all controllable loads in a single house based on TOU tariffs. Refs. [4,5] build DR control model for heating, ventilating and air conditioning (HVAC) system of one house. Ref. [6] presents a scheduling model for shiftable loads of household. Refs. [7,8] build a DR model for single house considering thermal storage system. Refs. [9–13] build specific DR models for HVAC, energy storage system (ESS), electric vehicle (EV), and shiftable loads respectively, and combine them to a complete DR model of single building. Ref. [14] presents a real-time DR management approach for household utilizing stochastic

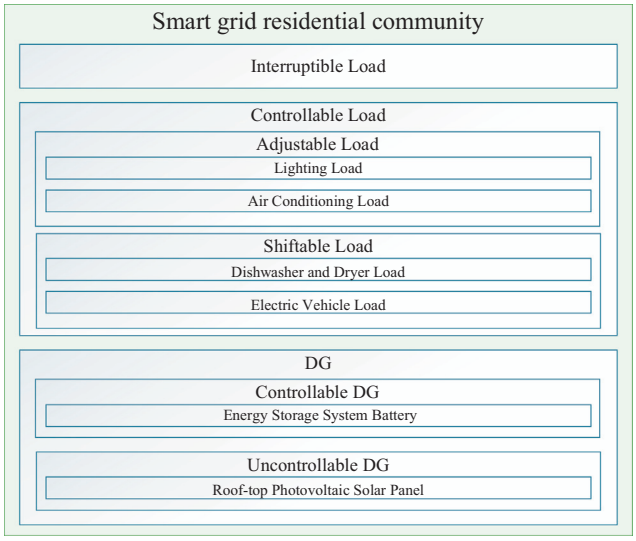

Fig. 1. Components of smart residential community load and distributed generation.

optimization and robust optimization. However, those studies did not consider the circumstances of scheduling the entire residential community that consists of numbers of households. Papers [15–20] discuss the centralized DR dispatch for one specific category of applications respectively. Refs. [15,16] study the DR control model for all HVACs in residential community. Ref. [17] presents a DR control approach for building heating systems. Ref. [18] studies the control strategy on the smart plug of residential load via signing contract with customers. Ref. [19] focuses on household distributed energy storage dispatch strategies, and Ref. [20] introduces an optimal scheduling for residential battery storage with solar PV. In addition, a technical and economical assessment has been done upon the storages installed to customer-side in [21]. Nevertheless, the works above did not involve the situation that contains multiple types of loads. Refs. [22–27] discuss the DR with multi households. Ref. [22] proposes a methodology for optimal bidding in a day-ahead market for micro grid incorporating the uncertainty of solar power, whereas the biding model is mainly focused on DG and the loads are assumed to be uncontrollable. Ref. [23] schedules residential power with three modes based on electricity cost and users' satisfaction of comfort, yet without providing detailed model of power applications. Ref. [24] presents an algorithm for distributed demand response, where residents are not aggregated and scheduled by LA. Ref. [25] presents a direct load control (DLC) approach for large-scale residential DR, which, however, is not suitable for day-ahead DR scheduling where price-based DR program and IL program are mainly employed. Studies in [26,27] focus on DR of residential energy hub where electric and natural gas loads are combined and managed optimally. However, the structure of smart residential community differs from that of residential energy hub, thus resulting in requests for a distinct DR scheme. Therefore, energy hub optimization approaches are not compatible for the smart residential community. In summary, there is not yet a particular scheme that entirely settles smart residential community DR problem where each particular load in household is aggregated and directly dispatched by LA.

At present, price-based and incentive-based DR programs are mainly TOU, CPP, RTP programs, and IL program respectively. This paper proposes a DR strategy for the newly built residential community in smart grid where residential loads are aggregated and directly dispatched by LA. The paper also presents an optimal scheduling model performed by LA and focusing on the DR programs above. Multiple load applications and DG in the community are modeled in detail and optimally scheduled. The proposed scheme can significantly exert the potential DR ability of the smart residential community. The model dramatically reduces the customer's electricity cost and decreases the peak load and peak-valley difference of residential load without bringing discomfort to the users. In addition, it can also provide support for decisions of electricity pricing strategies under power market development.

In the rest of this paper, firstly the loads in community based on various DR strategies are classified, and the optimum dispatch model is built in detail for interruptible and controllable loads. Secondly, a complete community DR scheduling model is formulated from the model above incorporating DR optimization of multiple DG. Lastly, the effectiveness of this model is simulated and confirmed on smart residential community of a smart grid application demonstration project in Suzhou, Jiangsu province, China., and the results of cases under different price-based DR programs are discussed.

2. Smart residential community DR scheduling model

According to the presence of price-based and incentive-based DR programs, this paper models the DR scheduling of residential community load considering IL combined with either TOU, CPP or RTP program. LA receives market day-ahead price signal and IL tariff at first. Then it optimizes the dispatch of residential load

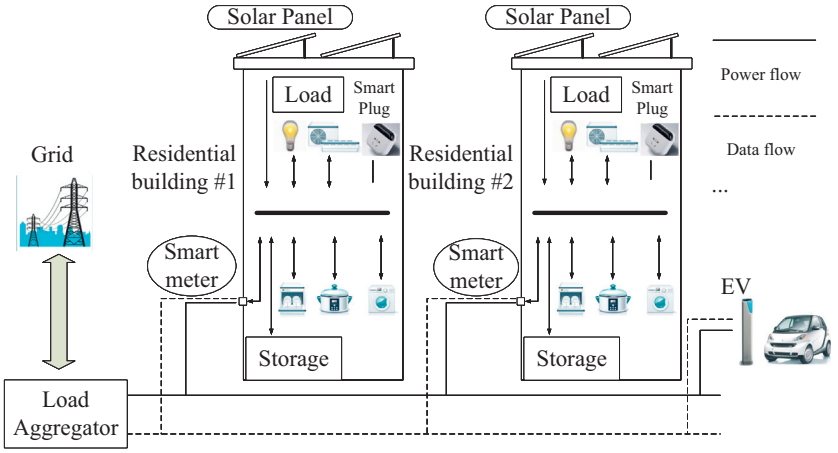

Fig. 2. Smart residential community DR structure.

via smart meters, and schedules the day-ahead (24 h) residential load curve.

In advance of the formulation of this problem, all the decision variables in this scheduling problem are defined and listed as follows:

Continuous variables:

Curtailed power of user j at hour t (kW) $P^{l}_{j,t}$;

Power of illumination load j at hour t (kW) $P^{a}_{j,t}$;

Air conditioner temperature of air conditioner k at hour t (°C) $T_{k,t}$;

Temperature adjustment of air conditioner k at hour t (°C) when it is turned on $T^{g}_{k,t}$;

Load power of air conditioner k at hour t (kW) $P^{a}_{k,t}$;

Temperature set point of air conditioner k at hour t (°C) $T^{s}_{k,t}$;

Load power of shiftable load j at hour t (kW) $P^{b}_{j,t}$;

Charge power of EV k at hour t (kW) $P^{b}_{k,t}$;

Power purchased from grid at hour t (kW) P^{g}_{t};

Battery change/discharge power of battery i at hour t (kW) $P^{S}_{i,t}$;

Discharge power/charge power of battery i at hour t (kW) $P_{d,i,t}$, $P_{c,i,t}$.

Binary variables:

Status indices of interruptible load j at hour t $I^{l}_{j,t}$;

Status indices of adjustment of illumination load j at hour t $I^{a}_{j,t}$;

Status indices of adjustment of air conditioner k at hour t $I^{a}_{k,t}$;

Status indices of shiftable load j at hour t $I^{b}_{j,t}$;

Charge status indices of EV k at hour t $I^{b}_{k,t}$;

Discharge/Charge binary status indices of battery i at hour t $I_{d,i,t}$, $I_{c,i,t}$.

2.1. Residential community load DR model

Residential loads are divided into three categories based on different DR strategies in this paper, which are interruptible load, adjustable load, and shiftable load. Interruptible load participates in DR through IL program. When the load responds, the total load power would drop for a large volume, which means the load is completely curtailed. Unlike interruptible load, adjustable load is not entirely curtailed during the response period, but decreases by small proportion of power instead, hence the load curve changes smoothly. Shiftable load differs from those two above. It does not reduce the total electricity consumption during DR program, but shifts the operation cycle duration optimally.

2.1.1. Interruptible load

This category of loads does not include controllable load appliance, so the loads are not responsive to the price-based DR program. In other words, these loads do not decrease when affected by electricity price, or can be shifted to low price hours. However, they can join the IL program through smart plug by signing contracts. Customers can choose which of their loads to join IL program voluntarily based on their own electricity usage habit. During load peak hours, when grid power supply is insufficient for load demand or electricity price is extremely high, customers would curtail partial load according to IL contract agreement. The interruptible load DR problem constraints are modeled as follows [28]. The curtailed power at each hour cannot exceed the maximum curtailable power and the original load power (1), (3). Total curtail hours are restricted by maximum daily curtailable hours (2).

$$0 \leqslant P^{l}_{j,t} \leqslant I^{l}_{j,t} P^{l,\max}_{j} \tag{1}$$

$$\sum_{t} I^{l}_{j,t} \leqslant X^{l,\max}_{j} \tag{2}$$

$$P^{l}_{j,t} \leqslant P^{L}_{j,t} \tag{3}$$

2.1.2. Adjustable load

Adjustable loads, such as illumination load, air conditioning load, etc., can adjust their power demand to participate in DR program. When hourly price is high, these loads would partially reduce power to a lower consumption level. Residents can set a price threshold value and power adjustment level to their adjustable loads based on their acceptable comfort. When the hourly real-time electricity price is higher than the price threshold, the power consumption level of load would decrease to a lower volume set by users. For instance, illumination load would dim brightness to the preset degree, and air conditioning load would adjust temperature set point to reduce power.

Illumination load DR problem constraints are modeled as follows:

$$P^{a}_{j,t} = P^{a,\text{base}}_{j,t}(1 - I^{a}_{j,t}) + P^{a,\min}_{j,t} I^{a}_{j,t} \tag{4}$$

$$\varepsilon\left(\rho_t - \rho^{a,\min}_{j,t}\right) < I^{a}_{j,t} \leqslant \varepsilon\left(\rho_t - \rho^{a,\min}_{j,t}\right) + 1 \tag{5}$$

When the real-time price ρ_t is higher than the price threshold $\rho^{a,\min}_{j,t}$, the binary status index of adjustment of illumination load $I^{a}_{j,t} = 1$ (5), and the illumination load power decreases from $P^{a,base}_{j,t}$ to $P^{a,\min}_{j,t}$ (4).

Air conditioning temperature state evolution is modeled with discrete time difference equation, which is commonly used in literatures [9,29] as follows:

$$T_{k,t+1} = \alpha_k T_{k,t} + (1 - \alpha_k)(T^{\alpha}_{k,t} - T^{g}_{k,t}) \tag{6}$$

$$\alpha_k = e^{-\Delta t / C_k R_k} \tag{7}$$

$$T^{g}_{k,t} = \begin{cases} R_k \eta_k P^{a}_{k,t} & \text{cooling mode} \\ -R_k \eta_k P^{a}_{k,t} & \text{heating mode} \end{cases} \tag{8}$$

$$P^{\min}_{k} \leqslant P^{a}_{k,t} \leqslant P^{\max}_{k} \tag{9}$$

$$T_{k,t} = T^{s}_{k,t} \tag{10}$$

The internal temperature of air conditioner at hour $t+1$ is described as a function of the internal temperature, ambient temperature, and the temperature adjustment at the hour t in (6). System inertia of air conditioner α_k is defined in (7). The transformation of air conditioner power to temperature adjustment is described in (8), and the air conditioner power is limited by its maximum and minimum value (9). The air conditioner internal temperature should be equal to the temperature set point (10).

This paper employs an adjustment control for air conditioner in cooling mode based on the model above and is formulated as follows, which can easily be modified for heating mode as well:

$$T^{s}_{k,t} = T^{s,\text{base}}_{k,t}(1 - I^{a}_{k,t}) + T^{s,\max}_{k,t} I^{a}_{k,t} \tag{11}$$

$$\varepsilon(\rho_t - \rho^{a,\min}_{k,t}) < I^{a}_{k,t} \leqslant \varepsilon(\rho_t - \rho^{a,\min}_{k,t}) + 1 \tag{12}$$

When the real-time price ρ_t is higher than the price threshold $\rho^{a,\min}_{k,t}$, the binary status index of adjustment of air conditioner $I^{a}_{k,t} = 1$ (12), and the temperature set point rises from $T^{s,\text{base}}_{k,t}$ to $T^{s,\max}_{k,t}$ (11).

2.1.3. Shiftable load

Operation duration time of these controllable loads can be shifted to low price period in accordance with the price signal. This paper divides shiftable load into two categories. One of them includes rice cooker, dryer, washing machine, and other similar loads. The other one is EV load.

2.1.3.1. Rice cooker and washing machine load. The feature of this type of load is that it consumes a fixed total amount of electric energy in a fixed period (i.e. cycle duration). Once the load is turned on, it will remain on for the duration of its cycles until it finishes one cycle. Although the load may consume different power volume at different time during the cycle (e.g. washing and drying stages of washing machine), the total quantity of energy consumption is fixed and cannot be divided into separate time periods. Therefore, a fixed average power is proposed to represent the power consumption amount at each hour of duration (13). The total energy usage can be represented as a product of average power multiplied by cycle duration time. Customers can set an operating time window (i.e. preferred start and end hours) for those loads. The load can be turned on at any time during the operating time window, and should be operated for one cycle during the operating time window (14)(16). The load DR problem constraints are formulated as follows:

$$P^b_{j,t} = P^{b,\text{average}}_j I^b_{j,t} \tag{13}$$

$$\left[X^{b,\text{on}}_{j,(t-1)} - U^b_j\right]\left[I^b_{j,(t-1)} - I^b_{j,t}\right] \geqslant 0 \tag{14}$$

$$X^{b,\text{on}}_{j,t} = \sum_{t=\tau}^{t} I^b_{j,t} \tag{15}$$

$$\sum_{t=\tau}^{T} I^b_{j,t} = \mathrm{U}^{\mathrm{b}}_{\mathrm{j}} \tag{16}$$

2.1.3.2. EV load. EV charge time window is from the home arrival time of the final trip in the day (i.e. EV plug-in time) to the departure time of the next day (i.e. end of charge time). Since EV actual charge duration is shorter than the time window, the decision of charging or not and the value of charging power at each hour can be made in (17). The state of charge (SOC) of EV at hour t $E^b_{k,t}$ is equal to the SOC at the last hour $E^b_{k,t-1}$ plus the charge power (18). EV should be fully charged in advance of customer's departure time (19). The EV's SOC at each hour is limited by its battery capacity (20).

$$P^{b,\min}_k I^b_{k,t} \leqslant P^b_{k,t} \leqslant P^{b,\max}_k I^b_{k,t} \quad (T_a \leqslant t \leqslant T_b) \tag{17}$$

$$E^b_{k,t} = E^b_{k,t-1} + P^b_{k,t}\Delta t / E^{\max}_k \tag{18}$$

$$E^b_{k,T_b} = 1 \tag{19}$$

$$E^b_{k,t} \leqslant 1 \tag{20}$$

In circumstance of multiple EVs in the community, the stochastic profile of the EV initial SOC E^b_{k,T_a} and home arrival time of the final trip T_a should be concerned. Residents' EV daily mileage is close to a logarithmic normal distribution. Besides, EV initial SOC is approximately linear related to its daily mileage. Thus, the probability density function of EV initial SOC can be obtained as follows [30]:

$$f(E^b_{k,T_a}) = \frac{1}{\sqrt{2\pi}D(1-E^b_{k,T_a})\sigma_d} \cdot \exp\left\{-\frac{\left[\ln(1-E^b_{k,T_a}) + \ln D - \mu_d\right]^2}{2\sigma_d^2}\right\} \tag{21}$$

where σ_d and μ_d are the mean and standard deviation parameters respectively. Home arrival time of the final trip T_a is close to a normal distribution curve. This paper uses a normal distribution function to describe the home arrival time of the community EVs [31,32].

2.2. Complete residential community DR scheduling model

In addition to electricity consuming load, renewable energy DG and ESS are also integrated to the smart residential community. On those of demand sides where photovoltaic solar panel is installed, solar power consumption takes precedence, and the residual load is supplied by both ESS and grid. The objective function of this model is to minimize the purchased electricity cost of residents (22).

$$\mathrm{Min}\sum_t \rho_t P^g_t - \sum_t \sum_j \rho^l_j P^l_{j,t} \tag{22}$$

The power of both demand side load and grid side supply should meet the power balance constraint (23).

$$\sum_i P^V_{i,t} + \sum_i P^S_{i,t} + P^g_t = \sum_j (P^L_{j,t} - P^l_{j,t}) + \sum_j P^a_{j,t} + \sum_k P^a_{k,t} + \sum_j P^b_{j,t} + \sum_k P^b_{k,t} \tag{23}$$

To prevent a large portion of load to be scheduled to low price hours which may create new peaks, the purchased grid power is restricted by (24).

$$P^{g,\min} \leqslant P^g_t \leqslant P^{g,\max} \tag{24}$$

Roof-top solar panels are uncontrollable DG. Since total residential load is considerably higher than solar power generation, this paper assumes all solar power is only used by the community instead of exported to the grid. The solar power output is considered as a constant input to the presented model in this paper.

ESS battery constraints are formulated as follows:

$$P^S_{i,t} = P_{d,i,t} - P_{c,i,t} \tag{25}$$

$$I_{d,i,t} + I_{c,i,t} \leqslant 1 \tag{26}$$

$$I_{c,i,t}P^{\min}_{c,i} \leqslant P_{c,i,t} \leqslant I_{c,i,t}P^{\max}_{c,i} \tag{27}$$

$$I_{d,i,t}P^{\min}_{d,i} \leqslant P_{d,i,t} \leqslant I_{d,i,t}P^{\max}_{d,i} \tag{28}$$

$$E_{i,t} = E_{i,(t-1)} - \left(P_{d,i,t} \cdot \frac{1}{\eta^S_i} - \eta^S_i P_{c,i,t}\right)\Delta t / E^{\max}_i \tag{29}$$

$$E^{\min}_i / E^{\max}_i \leqslant E_{i,t} \leqslant 1 \tag{30}$$

$$E_{i,0} = E_{i,NT} \tag{31}$$

When the battery discharges, it performances as a power source. On the other hand, when it charges, it acts as a load (25). Battery cannot charge or discharge at the same time (26). The battery hourly charge and discharge power are restricted by (27) and (28) respectively. Eqs. (29) and (30) are battery SOC constraints, namely, the battery cannot charge when its SOC reaches 1, or discharge when its SOC reaches the minimum value. The initial SOC is equal to the SOC at the end of the scheduling hour (31).

To sum up, LA schedules the residential community load and DG on the objective of minimizing total power purchase cost under different DR programs. This model optimizes the day-ahead (24 h) power scheduling of residential community considering IL combined with TOU or CPP or RTP. The complete model is formulated as follows:

$$\text{Min} \sum_t \rho_t P_t^g - \sum_t \sum_j \rho_j^l P_{j,t}^l \tag{22}$$

$$\text{s.t.} \begin{cases} (1)-(20) \\ (23)-(31) \end{cases}$$

This problem is a mixed integer linear programming (MILP) problem which is solved by CPLEX in this paper.

3. Case study

3.1. Case study description

The case study data are mainly acquired from smart residential community of a smart grid application demonstration project in Suzhou, Jiangsu Province, China. Suzhou city is located at southeast of China, where residential loads rise to high level during summer time. In order to examine the ultimate performance of the scheduling model, load data in July 25, 2016, which is considered as a typical summer day of Suzhou, have been chosen for the simulation. Each household is equipped with 3 smart meters connected with three categories of loads, namely interruptible loads, adjustable loads, and shiftable loads, respectively. The original interruptible load and the controllable load data are acquired from the smart meters. Solar power output is acquired from the historical data of the community. Total data of 200 households are selected for simulation. Since the smart community is a demonstration project, the parameters of the household loads are considered to be unified to accelerate the calculation in this case.

3.1.1. Interruptible load

Interruptible load curtailment tariff $\rho^l = 15$ (¥/kW h). Maximum IL curtail hours $X^{l,\max} = 2$ (h). Maximum IL daily curtailed power $P^{l,\max} = 100$ (kW h). The original interruptible load is shown in Fig. 3.

3.1.2. Adjustable load

3.1.2.1. Illumination load. When the hourly price is higher than the threshold $\rho^{a,\min} = 0.54$ (¥/kW h), illumination load at hour t reduces its power from $P_t^{a,base}$ (kW) by 20% to its minimum power $P_t^{a,\min}$ (kW). The original illumination load is shown in Fig. 4.

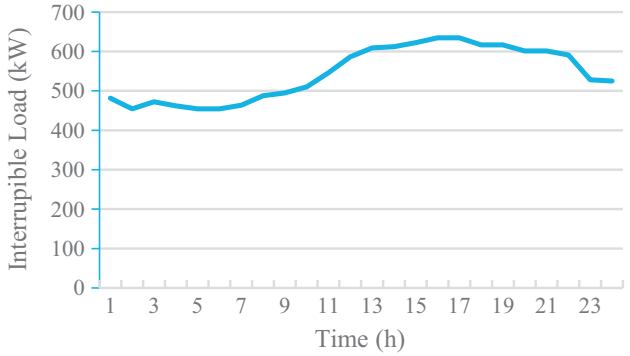

Fig. 3. Original interruptible load.

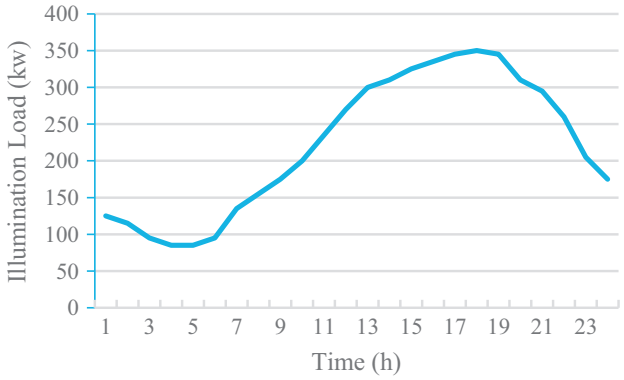

Fig. 4. Original illumination load.

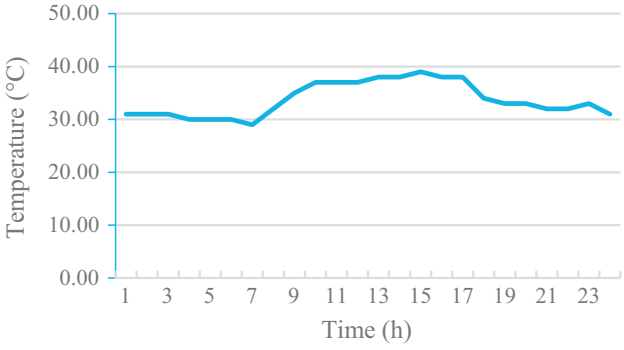

Fig. 5. Forecasted daily temperature.

3.1.2.2. Air conditioning load. The system inertia $\alpha = 0.82$, the thermal resistance $R = 2$ (°C/kW), the working efficiency factor $\eta = 2.5$, the maximum and minimum power of each air conditioner are 0 (kW) and 3.5 (kW) respectively, and the original temperature set point $T^{s,\text{base}} = 23$ (°C). When the hourly price is higher than the threshold $\rho^{a,\min} = 0.54$ (¥/kW h), the maximum temperature $T^{s,\max} = 24$ (°C). The number of air conditioners is 300. Forecasted daily temperature T_t^{α} is shown in Fig. 5.

3.1.3. Shiftable load

The numbers of rice cookers and washing machines are 200 respectively, and other data is listed in Table 1.

The EV maximum and minimum charge power $P_k^{b,\min}$, $P_k^{b,\max}$ are 0 (kW) and 3.3 (kW) respectively, the EV battery capacity $E_k^{\max} = 16$ (kW h), the EV maximum daily mileage $D = 40$ (mile), and the factors of EVs daily mileage logarithmic normal distribution density function are $\mu_d = 2.319$ and $\sigma_d = 0.88$. The EVs arrive home at different time according to a normal probability distribution function with the mean at 17:00 and the variance of 0.5 h. The end of charging time T_b is set to 24:00 (h), and the number of EVs is 100.

Table 1
Shiftable load data.

Shiftable load	Average power (kW)	Cycle duration (h)	User defined time window	
			Start time (h)	End time (h)
Rice cooker	1.5	2	16	20
Washing machine	0.6	1	9	17

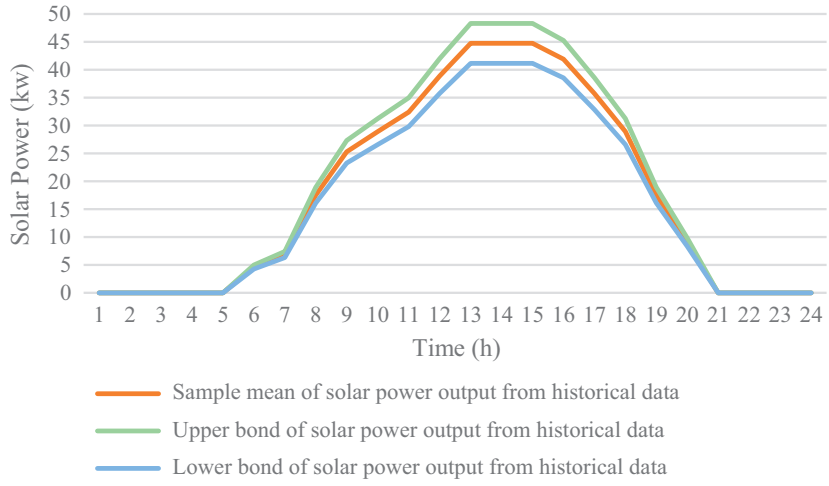

Fig. 6. Solar power output.

Table 2
Storage battery properties data.

Min charge/discharge power (kW)	0
Max charge/discharge power (kW)	150
Max stored energy (kW h)	500
Min stored energy (kW h)	100
Initial SOC	0.4
Inverter efficiency (charge/discharge)	85%/85%

3.1.4. DG

The sample mean of solar power based on the historical data of the community is considered as the actual solar power output in this case. The solar generation power of 24 h is shown in Fig. 6. The storage battery properties data are shown in Table 2.

3.1.5. Electricity price data

This paper studies 3 price-based DR programs, which are TOU, CPP, and RTP, in 3 cases respectively.

TOU: on-peak hours (15–18 h) price = 0.66 (¥/kW h), mid-peak hours (8–14 h and 19–20 h) price = 0.45 (¥/kW h), and off-peak hours (other hours) price = 0.21 (¥/kW h).
CPP: Critical-peak hours (15–18 h) price = 1.5 (¥/kW h), on-peak hours (12–14 h) price = 0.63 (¥/kW h), mid-peak hours (8–11 h and 19–20 h) price = 0.42 (¥/kW h), off-peak hours (other hours) price = 0.18 (¥/kW h).
RTP: Forecasted RTP price is shown in Fig. 7.

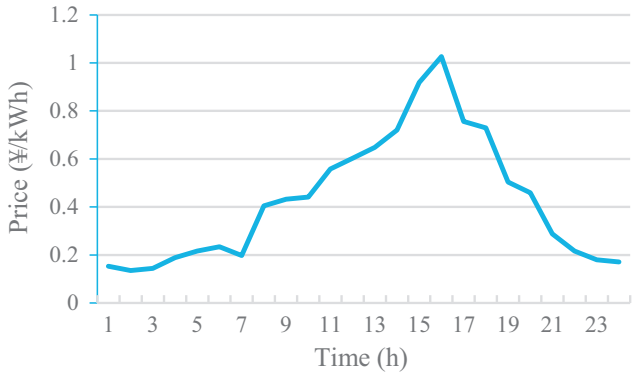

Fig. 7. Forecasted RTP price.

3.2. Case study results

This paper studies the stochastic properties of EV using Monte Carlo simulation by 1000 times in MATLAB. The simulation result displays the residential load curve under 3 different price-based DR programs. Firstly, the case of TOU is taken as instance for simulation by one time to study the community DR result of interruptible load, controllable load, and controllable DG respectively.

DR result of interruptible load participating in IL program is shown in Table 3. The load is curtailed by 100 kW at 17 h and 18 h respectively.

DR result of illumination load participating in TOU program is shown in Table 4. The total reduced energy consumption during on-peak hours (15–18 h) is 271kW h.

DR result of air conditioner participating in TOU program is shown in Fig. 8. The peak load reduces from 960 kW to 933 kW, and the time of peak appearance delays from 15th to 18th hour. The total air conditioning energy consumption is reduced by 180 kW h.

DR results of rice cooker and washing machine load participating in TOU program are shown in Table 5. Since the pre-set time window for washing machine is 9–17 h, the original start hour is at low price hour, hence the washing machine load is not shifted. However, the original rice cooker working hour starts at peak hour, therefore the load operation starting time is postponed by 3 h to mid-peak hour in the pre-set time window (16–20 h).

Table 3
Curtailment of Interruptible load participating in IL program.

Curtailed power (kW)	Load curtailment time (h)
100	17
100	18

Table 4
Adjustment of illumination load participating in TOU program.

Adjusted illumination load power (kW)	Load adjustment time (h)
65	15
67	16
69	17
70	18

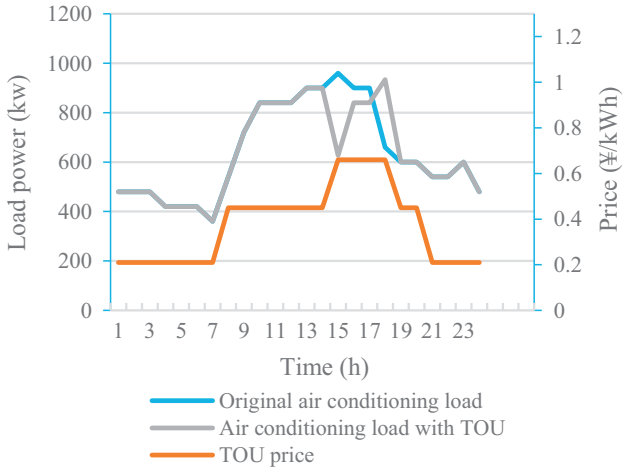

Fig. 8. Air conditioning load participating in TOU program.

Table 5
Time shift of rice cooker and washing machine load participating in TOU program.

	Operation start time (h)	Operation end time (h)
Original rice cooker load	16	17
Original washing machine load	9	9
Rice cooker load with TOU	19	20
Washing machine load with TOU	9	9

DR result of EV load participating in TOU program is shown in Fig. 9. Before participating in TOU program, EV load is mostly centralized in on-peak and mid-peak hours. When TOU is applied, 95.9% of the original load from on-peak and mid-peak hours is shifted to off-peak hours, which is a significant shift value.

DR result of battery storage participating in TOU program is shown in Fig. 10. The battery charges (i.e. negative power in the Fig. 10) during off-peak hours and discharges during on-peak hours, and managed to shave the peak and fill the valley of the demand side load curve.

Secondly, the DR scheduling results of the complete residential community are analyzed and discussed in 3 cases of IL combined with TOU, CPP, and RTP respectively.

Residential load curve without DR program is shown in Fig. 11.

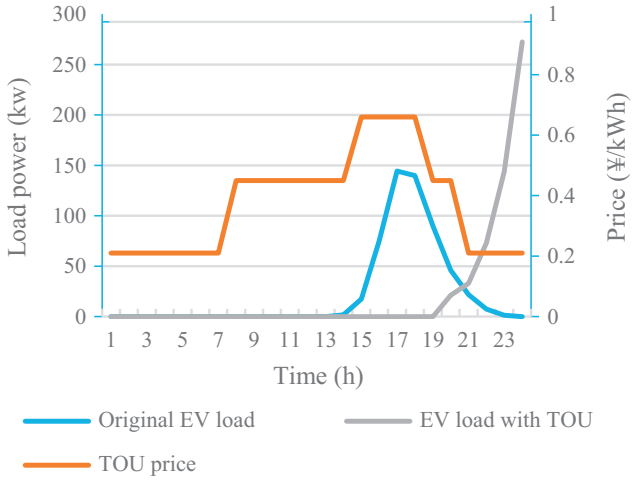

Fig. 9. EV load participating in TOU program.

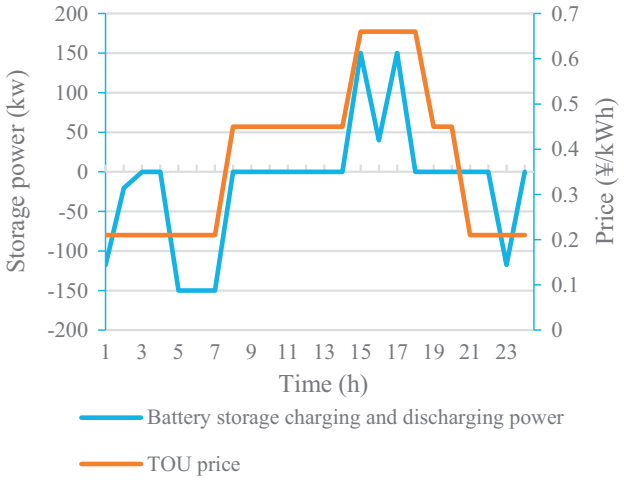

Fig. 10. Battery storage participating in TOU program.

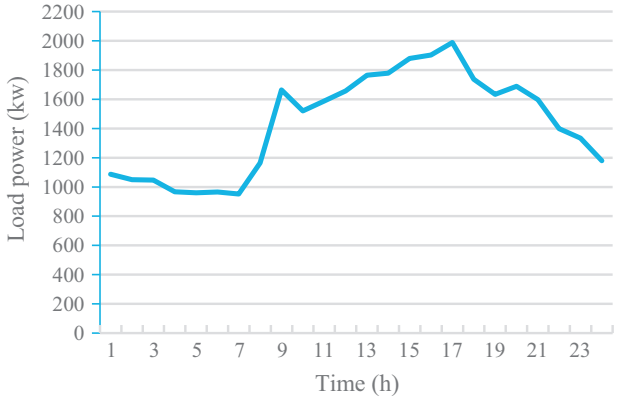

Fig. 11. Residential load without DR program.

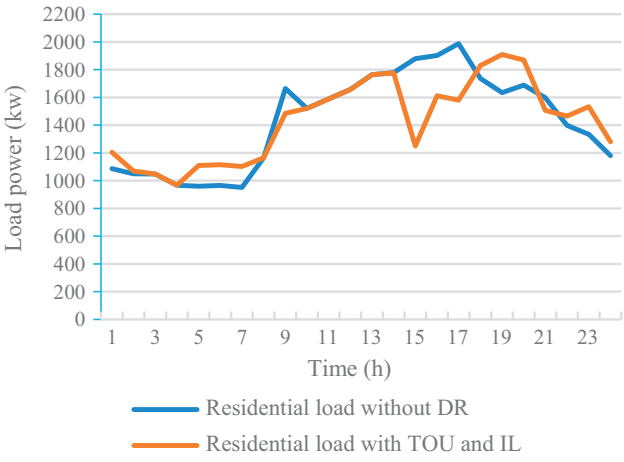

Fig. 12. Residential load with TOU and IL programs.

Case1: Residential load curve with TOU and IL programs is shown in Fig. 12. After participating in TOU and IL programs, the residential peak load decreases from 1988.21 kW to 1909.90 kW by 3.94%. Besides, the time of load peak appearance is shifted from 17th to 19th hour, and the peak-valley deference decreases from 1036.59 kW to 942.90 kW by 9.04%. The total energy consumption reduces by 0.29%, and the total power purchase cost is 10585.93¥.

Fig. 13. Residential load with CPP and IL programs.

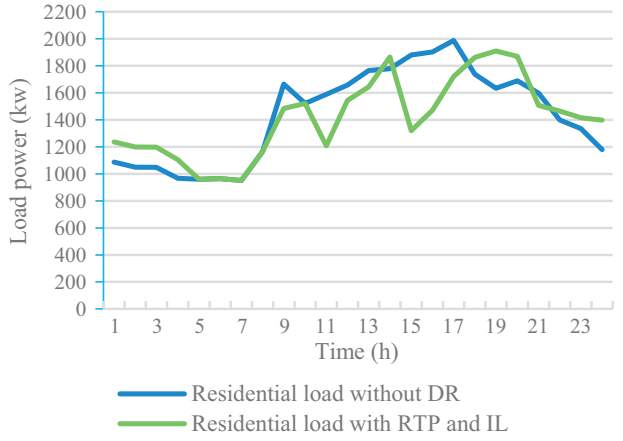

Fig. 14. Residential load with RTP and IL programs.

Case 2: Residential load curve with CPP and IL programs is shown in Fig. 13. After participating in CPP and IL programs, the peak load decreases to 1909.90 kW by 3.94%, and the time of load peak appearance is shifted from 17th to 19th hour. The peak-valley deference decreases to 942.60 kW by 9.04%. The community total energy consumption reduces by 1.07%, and the total power purchase cost is 15933.03¥.

Case 3: Residential load curve with RTP and IL programs is shown in Fig. 14. It is the same with case 1 and 2 that the peak load decreases to 1909.90 kW, the time of load peak appearance is shifted to 19th hour. However, the peak-valley deference decreases to 958.28 kW by 7.56%. In comparison to case 1 and 2, the community total energy consumption reduces by 1.52%, and the total power purchase cost is 12595.54¥.

3.3. Case analysis and discussion

It can be observed from the cases results above that the peak load and peak-valley difference are dramatically reduced in 3 cases respectively, where results in case 1 and 2 have superior performance than case 3. The load peak appearance time in cases are all shifted to 19th hour, which is beneficial to alleviate the power load of the grid in daylight. Fig. 15 shows the comparison of the total energy consumption and the total power purchase cost among 3 cases. According to the 3 cases results, although the peak load reductions are the same, the peak-valley deference decrement

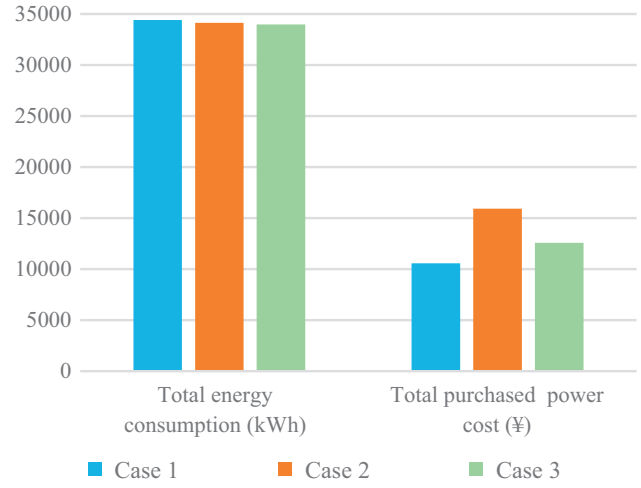

Fig. 15. Total energy consumption and the total power purchase cost of 3 cases.

in case 1 and 2 are more than case 3. The total energy consumption in case 3 is less than other cases. However, customers power purchase cost in case 1 is the lowest among 3 cases. Besides, in comparison to case 1, the load curves in case 2 and 3 are more volatile, which is not conducive for the generation with low ramping rate to respond load variation. In summary, it can be indicated from the results that the CPP and RTP program in this case study needs improvement to achieve superior DR result. The TOU combined with IL is the optimal DR program in this case, and the residential community optimally responds under this program.

4. Conclusions

The appearance of the smart residential community brings an unprecedented challenge to residential DR scheduling in power market. This paper presents a DR scheduling model for smart residential community based on the residential load dispatch through LA. The model optimally schedules the residential loads under different price-based DR programs combined with IL program. The objective of the model is to minimize the user's electricity consumption cost. It optimally schedules the entire community DR resources under different DR programs without interfering customers comfort, which reduces the user's cost of electricity, and simultaneously decreases the residential peak load, load peak-valley difference and energy consumption. The residential community's DR potentiality is significantly stimulated through this model. In addition, it can be noticed from the case study that analysis upon the scheduled load curves can be done to compare different DR programs, through which an optimal DR program can be decided. Therefore, the model can also provide support for electricity pricing scheme determination under electric power market development.

Acknowledgments

This work was supported by National Key R&D Program of China (2016YFB0901104) and National Natural Science Foundation of China (51577061).

References

[1] Rieger A, Thummert R, Fridgen G, Kahlen M, Ketter W. Estimating the benefits of cooperation in a residential microgrid: a data-driven approach. Appl Energy 2016;180:130–41.
[2] Siano P, Sarno D. Assessing the benefits of residential demand response in a real time distribution energy market. Appl Energy 2016;161:533–51.

[3] Pallonetto F, Oxizidis S, Milano F, Finn D. The effect of time-of-use tariffs on the demand response flexibility of an all-electric smart-grid-ready dwelling. Energy Build 2016;128:56–67.
[4] Yoon JH, Baldick R, Novoselac A. Dynamic demand response controller based on real-time retail price for residential buildings. IEEE Trans Smart Grid 2014;5:121–9.
[5] Yoon JH, Bladick R, Novoselac A. Demand response for residential buildings based on dynamic price of electricity. Energy Build 2014;80:531–41.
[6] Setlhaolo D, Xia XH, Zhang JF. Optimal scheduling of household appliances for demand response. Electr Power Syst Res 2014;116:24–8.
[7] Shafie-khah M, Kheradmand M, Javadi S, Azenha M, de Aguiar JLB, Castro-Gomes J, et al. Optimal behavior of responsive residential demand considering hybrid phase change materials. Appl Energy 2016;163:81–92.
[8] Alimohammadisagvand B, Jokisalo J, Kilpeläinen S, Ali M, Sirén K. Cost-optimal thermal energy storage system for a residential building with heat pump heating and demand response control. Appl Energy 2016;174:275–87.
[9] Paterakis NG, Erdinc O, Bakirtzis AG, Catalao JPS. Optimal household appliances scheduling under day-ahead pricing and load-shaping demand response strategies. IEEE Trans Ind Inform 2015;11:1509–19.
[10] Shao SN, Pipattanasomporn M, Rahman S. Development of physical-based demand response-enabled residential load models. IEEE Trans Power Syst 2013;28:607–14.
[11] Erdinc O, Paterakis NG, Mendes TDP, Bakirtzis AG, Catalao JPS. Smart household operation considering Bi-directional EV and ESS utilization by real-time pricing-based DR. IEEE Trans Smart Grid 2015;6:1281–91.
[12] Zhang D, Li SH, Sun M, O'Neill Z. An optimal and learning-based demand response and home energy management system. IEEE Trans Smart Grid 2016;7:1790–801.
[13] Sharma I, Dong J, Malikopoulos AA, Street M, Ostrowski J, Kuruganti T, et al. A modeling framework for optimal energy management of a residential building. Energy Build 2016;130:55–63.
[14] Chen Z, Wu L, Fu Y. Real-time price-based demand response management for residential appliances via stochastic optimization and robust optimization. IEEE Trans Smart Grid 2012;3:1822–31.
[15] Cole WJ, Rhodes JD, Gorman W, Perez KX, Webber ME, Edgar TF. Community-scale residential air conditioning control for effective grid management. Appl Energy 2014;130:428–36.
[16] Yin RX, Kara EC, Li YP, DeForest N, Wang K, Yong TY, et al. Quantifying flexibility of commercial and residential loads for demand response using setpoint changes. Appl Energy 2016;177:149–64.
[17] Bianchini G, Casini M, Vicino A, Zarrilli D. Demand-response in building heating systems: a model predictive control approach. Appl Energy 2016;168:159–70.
[18] Li WT, Yuen C, Ul Hassan N, Tushar W, Wen CK, Wood KL, et al. Demand response management for residential smart grid: from theory to practice. IEEE Access. 2015;3:2431–40.
[19] Zheng ML, Meinrenken CJ, Lackner KS. Smart households: dispatch strategies and economic analysis of distributed energy storage for residential peak shaving. Appl Energ. 2015;147:246–57.
[20] Ratnam EL, Weller SR, Kellett CM. Scheduling residential battery storage with solar PV: Assessing the benefits of net metering. Appl Energy 2015;155:881–91.
[21] Graditi G, Ippolito MG, Telaretti E, Zizzo G. Technical and economical assessment of distributed electrochemical storages for load shifting applications: an Italian case study. Renew Sustain Energy Rev 2016;57:515–23.
[22] Ferruzzi G, Cervone G, Delle Monache L, Graditi G, Jacobone F. Optimal bidding in a day-ahead energy market for micro grid under uncertainty in renewable energy production. Energy 2016;106:194–202.
[23] Ma K, Yao T, Yang J, Guan X. Residential power scheduling for demand response in smart grid. Int J Electr Power Energy Syst 2016;78:320–5.
[24] Fan Z. A distributed demand response algorithm and its application to PHEV charging in smart grids. IEEE Trans Smart Grid 2012;3:1280–90.
[25] Chen C, Wang JH, Kishore S. A distributed direct load control approach for large-scale residential demand response. IEEE Trans Power Syst 2014;29:2219–28.
[26] Rastegar M, Fotuhi-Firuzabad M. Load management in a residential energy hub with renewable distributed energy resources. Energy Build 2015;107:234–42.
[27] Brahman F, Honarmand M, Jadid S. Optimal electrical and thermal energy management of a residential energy hub, integrating demand response and energy storage system. Energy Build 2015;90:65–75.
[28] Sahebi MM, Duki EA, Kia M, Soroudi A, Ehsan M. Simultanous emergency demand response programming and unit commitment programming in comparison with interruptible load contracts. IET Gener Transm Dis. 2012;6:605–11.
[29] Mathieu JL. Lawrence Berkeley Nat. Lab. Modeling, analysis, and control of demand response resources. Ph.D. dissertation. http://escholarship.org/uc/item/7pm9p24f; 2013 [accessed 17.02.22].
[30] Cai DF, Qian B, Chen JF, Yao MQ. Analysis on dynamic probabilistic characteristic of power grid connected with electric vehicle charging load and wind power. Power System Technol 2013;3:590–6 [in Chinese].
[31] Taylor J, Maitra A, Alexander M, Brooks D, Duvall M. Evaluation of the impact of plug-in electric vehicle loading on distribution system operations. IEEE Pow Ener Soc Ge 2009:2076–81.
[32] Shao SN, Pipattanasomporn M, Rahman S. Grid integration of electric vehicles and demand response with customer choice. IEEE Trans Smart Grid 2012;3:543–50.